

## Observation of Magnetophonon Resonance of Dirac Fermions in Graphite

Jun Yan,<sup>1,\*</sup> Sarah Goler,<sup>2</sup> Trevor D. Rhone,<sup>1</sup> Melinda Han,<sup>1</sup> Rui He,<sup>1</sup> Philip Kim,<sup>1</sup> Vittorio Pellegrini,<sup>2</sup> and Aron Pinczuk<sup>1</sup>

<sup>1</sup>*Department of Physics and Department of Applied Physics and Applied Mathematics, Columbia University, New York, New York 10027, USA*

<sup>2</sup>*NEST Istituto Nanoscienze CNR and Scuola Normale Superiore, I-56127, Pisa, Italy*

(Received 6 August 2010; published 24 November 2010)

Coherent coupling of Dirac fermion magnetoexcitons with an optical phonon is observed in graphite as marked magnetic-field dependent splittings and anticrossing behavior of the two coupled modes. The sharp magnetophonon resonance occurs in regions of the graphite sample with properties of superior single-layer graphene having enhanced lifetimes of Dirac fermions. The greatly reduced carrier broadening to values below the graphene electron-phonon coupling constant explains the appearance of sharp resonances that reveal a fundamental interaction of Dirac fermions.

DOI: 10.1103/PhysRevLett.105.227401

PACS numbers: 78.67.Wj, 78.30.-j, 78.20.Ls

The quest for ultra-high-quality graphene, the new celebrated two-dimensional (2D) electron gas [1], is driven by expectations of discoveries of novel physics and applications linked to massless Dirac fermions [2,3]. A crucial parameter that sets the quality of the graphene layer is the lifetime of Dirac fermions. An enhanced lifetime would enable manifestations of quantum coherent coupling effects even when the relevant interaction strengths are rather weak. A class of such coherent phenomena is linked to the (weak) coupling of the particle-hole transitions between  $\pi^*$  (conduction) and  $\pi$  (valence) bands of the Dirac cone with optical phonons [4,5] resonantly tuned by an external magnetic field [6,7].

These resonant coupling phenomena (magnetophonon resonances or MPR) occur when the energy spacing between Landau levels (LLs) is continuously tuned to cross the energy of an optical phonon mode. MPRs have been explored in bulk semiconductor materials [8–10], in two-dimensional semiconductor systems and in quantum dots [11,12].

Recent theoretical studies in graphene have suggested that MPR leads to a rich splitting and anticrossing phenomena of the even parity  $E_{2g}$  long wavelength optical mode due to its MPR interactions with excitations across Dirac fermion LLs (magnetoexcitons) [6,7].

The experimental manifestation of MPR relies on a delicate interplay between the lifetimes of Dirac fermion modes and the electron-phonon coupling. A magnetic-field tunable anomaly in the optical phonon of graphene has been reported [13,14]. In these works the resolution of the anticrossing that is the signature of the coherent coupling of electron-phonon modes is impeded by the relatively short lifetimes of the fermion excitations. The manifestation of the sharp MPR requires damping of the Dirac fermion excitations well below the weak electron-phonon coupling. This qualitatively new regime of interacting Dirac fermion modes has not been achieved so far.

In this Letter we demonstrate the coherent mixing of the  $E_{2g}$  phonon and the Dirac fermion magnetoexciton mode

that is the essence of the MPR. At selected values of the magnetic field we observe the emergence of two distinct modes displaying the characteristic anticrossing behavior. These observations uncover unprecedented narrow linewidths of Dirac fermion magnetoexciton transitions. The Landau level transition Lorentzian widths of 3.2 meV reported here are about 3 times smaller than those of previous investigations at similar magnetic fields [14–16] and yield damping values below the graphene electron-phonon coupling constant. Surprisingly, the enhanced Dirac fermion lifetimes required for the observations of the characteristic MPR electron-phonon mode anticrossings are found in selected regions of graphite.

We show below that our findings can be modeled with a simple coupled mode Hamiltonian describing the  $E_{2g}$  mode and sharp magnetoexcitons of a graphene layer. The sharp Landau level transitions found in this work and the interpretation in terms of a single-layer graphene model are in line with recent experimental and theoretical studies that suggest the existence of high-quality decoupled graphene flakes in bulk graphite [15,17,18]. In our work the unique areas are identified by the capability to scan regions of the sample within the environment of the magneto-optics experiment. Consistent with this interpretation, our spatially resolved Raman analysis reveals a large nonuniformity of the graphite sample and areas of the sample where no MPRs are identified (see supplementary material [19]).

The main MPR is found close to 5 T and involves the  $-1 \rightarrow 2$  and  $-2 \rightarrow 1$  Landau level transitions of Dirac fermions [Landau levels in the  $\pi^*$  ( $\pi$ ) band correspond to the positive (negative) integers] as shown in Fig. 1(a). Representative examples of spectra showing the two coupled modes  $\omega_-$  and  $\omega_+$  are presented in Figs. 1(c) and 1(d) together with the magnetic-field evolution of the expected mode anticrossing behavior [Fig. 1(b)]. The simple coupled mode physics underlying the data enables algebraic extraction of parameters of the interacting system including the Dirac fermion lifetimes.

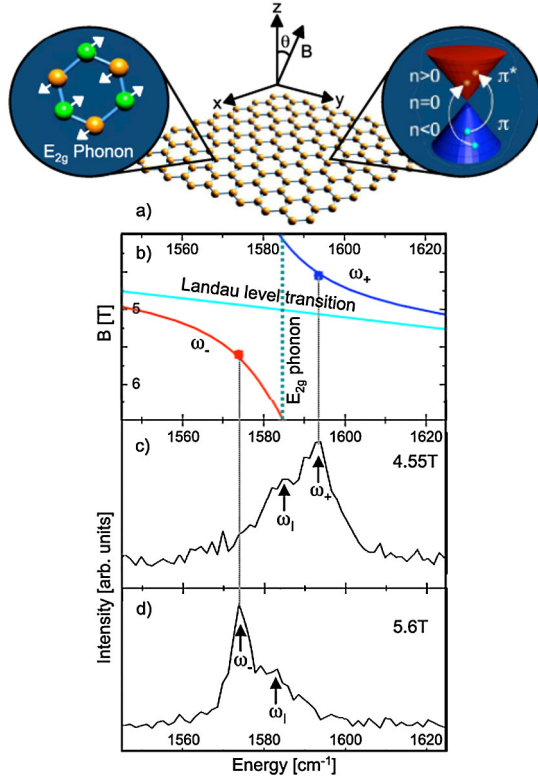


FIG. 1 (color online). (a) Schematic visualizations of the phonon and magnetoexciton modes involved in the magnetophonon resonance (MPR). The graphene layer is illustrated in the  $x$ - $y$  plane. The magnetic-field direction in the experiment is tilted by  $\theta = 20^\circ$  from the  $z$  axis. (b) Energies of two coupled normal modes versus magnetic field close to the MPR at around  $B = 5$  T. (c) and (d) Raman spectra acquired at 4.55 and 5.6 T, respectively. The energies of the two coupled modes  $\omega_-$  and  $\omega_+$  are indicated by the two dots in panel (b). The origin of the additional peak  $\omega_1$  is discussed later in the text.

Raman experiments were performed at 2 K in a magnetic field up to 14 T in a backscattering configuration with a tilt angle of  $\theta = 20^\circ$  between the magnetic field and the  $c$ -axis direction of Kish graphite (Toshiba ceramics) which was deposited onto a Si/SiO<sub>2</sub> substrate [see Fig. 1(a)]. A diode-pumped solid-state laser with a 532 nm emission line was used as the excitation source and focused on the sample with a spot size of about 80  $\mu\text{m}$  and a power of around 30 mW. The laser spot was moved around on the sample to select regions with optimized MPR responses. We also performed micro-Raman measurements (spatial resolution of 0.5  $\mu\text{m}$ ) at room temperature in air on different pieces of the sample which exhibits large spatial variations of the 2D band (see supplementary material [19]).

Figure 2 displays the magnetic-field dependence of the Raman spectra that we obtained on two different spots of the sample. The  $E_{2g}$  phonon displays drastically different behavior. In Fig. 2(a) the spectra are very sensitive to the tuning of the magnetic field, while in Fig. 2(b) no changes are observed. This highlights the nonuniformity of the

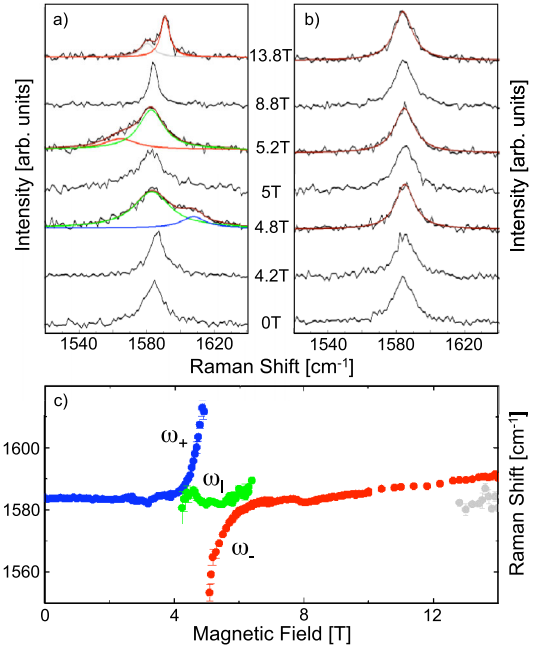


FIG. 2 (color online). (a) and (b) Magnetic-field dependence of the  $E_{2g}$  phonon spectra taken at two representative regions of the sample. One region displays significant MPR effect while the other does not. The smooth curves are Lorentzian fits to the data. (c) Mode energy evolution extracted from the spectra displayed in (a).

graphite and the presence of regions that behave like single-layer graphene as further supported by the spatially dependent analysis of the 2D band Raman spectra (see supplementary material [19]). We link the MPR to regions of the graphite sample where there is a significant contribution to the Raman spectra from decoupled graphene layers. Furthermore, while we only reproducibly measured MPR of one Kish graphite sample, the nonuniformity of the 2D band was observed in many graphite samples by us as well as other groups [20]. Behavior similar to that in Fig. 2(b) has been reported and ascribed to the usual Bernal stacked graphite [14]. Below we will focus on the remarkable data displayed in Fig. 2(a).

The magnetic-field evolution of the mode energies of these spectra are shown in Fig. 2(c). Previous studies have observed a phonon energy modulation of about 40  $\text{cm}^{-1}$  using magnetic fields up to 30 T [14]. Here we found the optical phonon energy is modulated by more than 60  $\text{cm}^{-1}$  with fields less than 6 T, indicating the presence of very high-quality Dirac fermions with long lifetimes.

The extreme sensitivity of the spectral line shape to magnetic-field changes seen in Fig. 2(a) suggests the existence of LL transitions that come into and out of resonance with the phonon energy. It is also remarkable that at  $\sim 6.5$  Tesla the phonon becomes extremely sharp, with a width of 4  $\text{cm}^{-1}$ . To the best of our knowledge this is the narrowest  $E_{2g}$  phonon width reported in graphene-related materials.

Electric-field effect studies have shown that a sharp  $E_{2g}$  phonon is linked to the absence of resonant electron-hole pair transition states that the lattice vibration can decay into [4,5,21]. This indicates that at around 6.5 T no LL transition exists that resonantly interacts with the phonon. It follows that observations of a very sharp phonon have a nontrivial implication on the LL structure of the underlying electronic system. Furthermore, the significant line shape changes around 5 T suggest that a LL transition with large degeneracy comes into resonance with the long wavelength optical phonon. Comparing with current LL studies of graphitic materials [22–24], the transition matches well with the  $-1 \rightarrow 2$  (and  $-2 \rightarrow 1$ ) transitions of Dirac fermions. Based on these considerations we proceed to model the electron system in the MPR anticrossing displayed in Figs. 2(a) and 2(c) as Dirac fermions with discrete LL structures characteristic of those in single-layer graphene of high perfection.

Figure 3 shows the detailed evolution of the phonon spectrum. We observe that the line shape is very asymmetric and the asymmetry changes side when crossing 5 T. As shown, all the asymmetric spectra can be decomposed into two Lorentzian peaks.

The two modes which we highlight in the figure form a paired behavior at about 5 T. Taking into account the  $20^\circ$  angle between the magnetic field and the graphite  $c$  axis, at resonance the field perpendicular to the basal plane is 4.7 T. The resonance condition of the  $-1 \rightarrow 2$  LL transition of

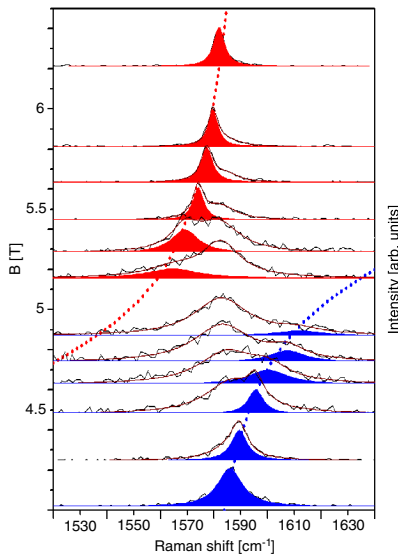


FIG. 3 (color online). Detailed Raman spectra of the main MPR observed for magnetic fields ranging from 4.2 to 6.4 T. The theoretical calculation of the anticrossing associated to the magnetophonon resonance (MPR) at 5 T (see text) is indicated by dotted lines. The spectral component that corresponds to the two coupled modes is highlighted. The spectra are shifted vertically so that each component taken at a given magnetic field has its peak aligned at that magnetic field.

Dirac fermions gives  $(1 + \sqrt{2})\frac{\sqrt{2}\hbar v_F}{l_B} = 196$  meV where  $l_B$  is the magnetic length, 196 meV is the  $E_{2g}$  phonon energy. This determines the Fermi velocity  $v_F$  to be  $1.03 \times 10^6$  m/s, in good agreement with studies of Dirac fermions in graphitic materials.

The mode energy and linewidth obtained from the analysis are displayed in Fig. 4. The splitting of the two anti-crossing branches asymptotically approaches a large value of  $70 \text{ cm}^{-1}$  at the resonance field of 5 T. This is in contrast with results in Fig. 2(b) and the studies reported in Ref. [14], in which the impact of the LL transition is seen largely as a weak perturbation that only weakly renormalizes the phonon energy and broadens the phonon Raman peak. In the results shown in Fig. 4, the sharpness of the LL transition leads to the strong mixing of the optical phonon with a magnetoexciton, and to the establishment of two distinct new collective modes that have characteristic anticrossing behavior.

To quantitatively analyze our data, we employ a coupled mode theory that was proposed by Goerbig *et al.* in Ref. [7] where the two coupled normal modes are described as

$$\hbar \omega_{\pm} = \frac{E_{\text{PH}} + E_{\text{ME}}}{2} \pm \sqrt{\left(\frac{E_{\text{PH}} - E_{\text{ME}}}{2}\right)^2 + g^2}. \quad (1)$$

In the equation,  $E_{\text{PH}}$  and  $E_{\text{ME}}$  describe the phonon and magnetoexciton, respectively, while  $g$  is the coupling parameter. To explicitly describe the broadening of the

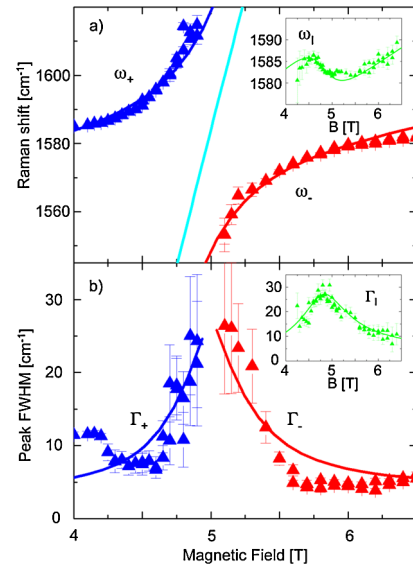


FIG. 4 (color online). MPR induced anticrossing behavior of the coupled modes. The two upper and lower lines in (a) are the theoretical fits of the energy of the two branches while the line in the middle is the Landau level transition  $-1 \rightarrow 2$  or  $-2 \rightarrow 1$ . The two lines in (b) correspond to the full-width-at-half-maximum (FWHM) of the coupled modes. The triangles are the experimental data. The inset reports the magnetic-field evolution of the  $\omega_+$  mode.

modes, we let  $E_{\text{PH}} = \omega - i\gamma$ ,  $E_{\text{ME}} = \Omega - i\Gamma$ , where  $\omega$ ,  $\Omega$ ,  $\gamma$ , and  $\Gamma$  are energies and half-widths of the phonon and magnetoexciton.

At resonance  $\omega = \Omega$ ,  $\hbar\omega_{\pm}^r = \omega \pm \sqrt{g^2 - (\frac{\Gamma-\gamma}{2})^2} - i\frac{\Gamma+\gamma}{2}$ . The phonon width  $\gamma$  in the absence of Landau damping into electron-hole pairs is  $4 \text{ cm}^{-1}$  so  $\gamma = 2 \text{ cm}^{-1}$ . The analysis using data in Fig. 4 yields the energy and broadening of the two coupled modes at resonance:  $\hbar\omega_{+}^r = (1619 - i14) \text{ cm}^{-1}$  and  $\hbar\omega_{-}^r = (1549 - i14) \text{ cm}^{-1}$ . These experimental data allow us to algebraically determine all the parameters in the coupled mode Hamiltonian:  $\omega = 1584 \text{ cm}^{-1}$ ,  $\Gamma = 26 \text{ cm}^{-1}$ , and  $g = 37 \text{ cm}^{-1}$ .

The value of  $g$  provides a direct measurement of the electron-phonon coupling strength since it is directly linked to the dimensionless electron-phonon coupling constant  $\lambda$  [6] by  $g = \sqrt{\frac{\lambda}{2}}\hbar\omega_B$  where  $\hbar\omega_B = \frac{\sqrt{2}\hbar v_F}{l_b}$ . Using the experimental result  $(\sqrt{2} + 1)\hbar\omega_B = \frac{1619+1549}{2} \text{ cm}^{-1}$ , we find  $\lambda = 6.36 \times 10^{-3}$ . Physically, this coupling strength reflects the modulation rate of the nearest neighbor hopping integral  $\gamma_0$  with respect to the stretching of the carbon-carbon bond length  $b$  and we obtain  $\frac{d\gamma_0}{db} = 6.66 \text{ eV}/\text{\AA}$ . These values are in reasonable agreement with experiments on monolayer graphene [25] and epitaxial graphene [14].

The Landau level transition half-width of  $26 \text{ cm}^{-1}$  (roughly  $3 \text{ meV}$ ) is an important indication that the Dirac fermions residing in graphite are of a very high degree of perfection. As a comparison, in epitaxial graphene with a reported mobility of  $250\,000 \text{ cm}^2/(\text{V} \cdot \text{s})$  [16], the Landau level width at  $5 \text{ T}$  is about  $10 \text{ meV}$ .

The narrow width  $\Gamma$  less than  $g$ , a condition not met before, allows for the coherent coupling between the phonon and the fermion excitations leading to the anticrossing phenomenon seen in our data. This observation opens further venues for fundamental research on Dirac fermions.

We now briefly discuss the green mode labeled  $\omega_I$  with energy and width displayed in the insets to Fig. 4. The behavior of this mode is quite similar to the magnetic oscillations observed in Ref. [14]. Interestingly, we found that the resonance field of  $\omega_I$  is slightly lower (at  $4.8 \text{ T}$ ) than that of the two anticrossing modes (at  $5 \text{ T}$ ). This might indicate disorder-induced Fermi velocity renormalization of graphene. The existence of the  $\omega_I$  mode is a further indication of sample nonuniformity.

For the magnetic-field range below  $4 \text{ T}$ , magnetophonon resonance with interband transitions of higher LL indexes are expected. However, we were unable to clearly identify such resonances, possibly due to the smaller LL degeneracy as well as limitations imposed by our signal to noise ratio detection limit.

Starting at about  $13 \text{ T}$ , the phonon splits again indicating the occurrence of another anticrossing [Fig. 2(c)]. This

resonance could be due to the  $0 \rightarrow 2$  LL transition that is expected at  $14.6 \text{ T}$  or the  $0 \rightarrow 1$  transition expected at  $29.1 \text{ T}$ . Because the resonance is incomplete, we are unable to rule out one or the other unambiguously.

We thank V. Piazza for assistance in the spatially resolved measurements. This work is supported by ONR (N000140610138 and Graphene MURI), by NSF (CHE-0641523), and the NYSTAR. P.K. acknowledges support from the FENA MARCO Center. A. P. is supported by NSF (DMR-0803691), and a grant from the Keck Foundation. V.P. is supported by a grant of the Ministry of Foreign Affairs (Italy).

\*Current address: Department of Physics, University of Maryland, College Park, MD, USA.

- [1] A. K. Geim and K. S. Novoselov, *Nature Mater.* **6**, 183 (2007).
- [2] X. Du *et al.*, *Nature (London)* **462**, 192 (2009).
- [3] K. I. Bolotin *et al.*, *Nature (London)* **462**, 196 (2009).
- [4] J. Yan *et al.*, *Phys. Rev. Lett.* **98**, 166802 (2007).
- [5] S. Pisana *et al.*, *Nature Mater.* **6**, 198 (2007).
- [6] T. Ando, *J. Phys. Soc. Jpn.* **76**, 024712 (2007).
- [7] M. O. Goerbig *et al.*, *Phys. Rev. Lett.* **99**, 087402 (2007).
- [8] D. R. Leadley *et al.*, *Phys. Rev. Lett.* **73**, 589 (1994).
- [9] D. J. Barnes *et al.*, *Phys. Rev. Lett.* **66**, 794 (1991).
- [10] E. J. Johnson and D. M. Larsen, *Phys. Rev. Lett.* **16**, 655 (1966).
- [11] Y. J. Wang *et al.*, *Phys. Rev. Lett.* **79**, 3226 (1997).
- [12] S. Hameau *et al.*, *Phys. Rev. Lett.* **83**, 4152 (1999).
- [13] J. Yan *et al.*, *Bulletin of the American Physical Society, 2009 APS March Meeting* (American Physical Society, New York, 2009), Vol. 54, <http://meetings.aps.org/Meeting/MAR09/Event/97585>.
- [14] C. Faugeras *et al.*, *Phys. Rev. Lett.* **103**, 186803 (2009).
- [15] G. Li, A. Luican, and E. Y. Andrei, *Phys. Rev. Lett.* **102**, 176804 (2009).
- [16] M. Orlita *et al.*, *Phys. Rev. Lett.* **101**, 267601 (2008).
- [17] P. Neugebauer *et al.*, *Phys. Rev. Lett.* **103**, 136403 (2009).
- [18] J. M. B. Lopes dos Santos, N. M. R. Peres, and A. H. Castro Neto, *Phys. Rev. Lett.* **99**, 256802 (2007).
- [19] See supplementary material at <http://link.aps.org/supplemental/10.1103/PhysRevLett.105.227401> for spatially resolved Raman analysis of the 2D phonon peak in Kish graphite.
- [20] I. Luk'yanchuk, Y. Kopelevich, and M. El Marssi, *Physica (Amsterdam)* **404B**, 404 (2009).
- [21] T. Ando, *J. Phys. Soc. Jpn.* **75**, 124701 (2006).
- [22] W. W. Toy, M. S. Dresselhaus, and G. Dresselhaus, *Phys. Rev. B* **15**, 4077 (1977).
- [23] M. Orlita *et al.*, *Phys. Rev. Lett.* **100**, 136403 (2008).
- [24] M. Orlita *et al.*, *Phys. Rev. Lett.* **102**, 166401 (2009).
- [25] J. Yan *et al.*, *Solid State Commun.* **143**, 39 (2007).